Amorphous and crystalline ices studied by dielectric spectroscopy

L. J. Plaga (iD), A. Raidt, V. Fuentes Landete, K. Amann-Winkel (iD), B. Massani (iD), T. M. Gasser, C. Gainaru (iD), T. Loerting (iD), and R. Böhmer (iD)

View Online   Export Citation   CrossMark

ARTICLES YOU MAY BE INTERESTED IN

Amorphous and crystalline ices studied by dielectric spectroscopy

L. J. Plaga,[1] (iD) A. Raidt,[1] V. Fuentes Landete,[2] K. Amann-Winkel,[2,a] (iD) B. Massani,[2,b] (iD) T. M. Gasser,[2]
C. Gainaru,[1] (iD) T. Loerting,[2] (iD) and R. Böhmer[1] (iD)

AFFILIATIONS

[1] Fakultät Physik, Technische Universität Dortmund, D-44221 Dortmund, Germany
[2] Institute of Physical Chemistry, University of Innsbruck, A-6020 Innsbruck, Austria

Note: This paper is part of a JCP Special Topic on Chemical Physics of Supercooled Water.
[a] **Current address:** Department of Physics, AlbaNova University Center, 10691 Stockholm, Sweden.
[b] **Current address:** SUPA, School of Physics and Astronomy and Centre for Science at Extreme Conditions,
The University of Edinburgh, Edinburgh EH9 3FD, United Kingdom.

ABSTRACT

This work reports on frequency dependent ambient-pressure dielectric measurements of hyperquenched glassy water, ice IV, ice VI, as well as a CO_2-filled clathrate hydrate, the latter featuring a chiral water network. The dipolar time scales and the spectral shapes of the loss spectra of these specimens are mapped out and compared with literature data on low-density and high-density amorphous ices as well as on amorphous solid water. There is a trend that the responses of the more highly dense amorphous ices are slightly more dynamically heterogeneous than those of the lower-density amorphous ices. Furthermore, practically all of the amorphous ices, for which broadband dielectric spectra are available, display a curved high-frequency wing. Conversely, the high-frequency flanks of the nominally pure ice crystals including ice V and ice XII can be characterized by an approximate power-law behavior. While the spectral shapes of the nominally pure ices thus yield some hints regarding their amorphicity or crystallinity, a comparison of their time scale appears less distinctive in this respect. In the accessible temperature range, the relaxation times of the crystalline ices are between those of low-density and high-density amorphous ice. Hence, with reference also to previous work, the application of suitable doping currently seems to be the best dielectric spectroscopy approach to distinguish amorphous from crystalline ices.

I. INTRODUCTION

The microscopic understanding of water's polyamorphism and glass transition and whether and how they might be related to many of the anomalies of H_2O continues to generate lively scientific debates.[1–3] One of the most controversial questions is whether the kinetic freezing or unfreezing experimentally observed near that transition involves translational motion of the oxygen atoms or rather essentially only proton transfer processes or molecular reorientations or a two-step scenario with rotations and translations taking place on different time scales.[4,5] An issue that apparently adds to the complexity of the situation is that there are so many different routes giving access to glassy states of H_2O with the question

arising how similar or different the microstructures and mesostructures as well as the dynamical properties of the variously vitrified waters are.[6–8]

Amorphous ices with a density somewhat below 1 g/cm³ can, for instance, be produced by deposition of H_2O vapor on a cryogenic substrate, thus leading to amorphous solid water (ASW)[6,9,10] or by splat-cooling of micrometer-sized liquid droplets to obtain hyperquenched glassy water (HGW).[7,11] By starting from the solid, i.e., from hexagonal ice (I_h), a suitable pressure/temperature protocol yields low-density amorphous (LDA) ice.[12] Dedicated compression routes also allow one to prepare high-density amorphous (HDA) and very-high-density amorphous (VHDA) forms[13–17] with debates as to whether and which of these more compact forms are

to be viewed as separate glassy states or not.[18,19] The possibility has even been raised that some amorphous states might be considered as "derailed" crystals.[20] Pressure collapsed clathrates, i.e., crystalline nanoporous water frameworks that are filled with suitable small-molecule guests, were investigated in this context as well.[21,22]

In efforts to unravel the complex structures of the various amorphous ices, a large number of diffraction investigations were conducted over the years.[23,24] Concerning the study of the glass transition, which typically features weak and sometimes even barely detectable thermodynamic signatures, calorimetric experiments are often used.[25-30] By virtue of wide-angle neutron scattering, the glass transition of ASW could be identified from the termination of its micropore collapse as well. Hill *et al.*[31,32] argued that without translational water motion, this latter phenomenon is inconceivable. With reference to previous work on ASW,[33] this collapse appears not to be driven by a possible "filling" of the micropores with small molecules.

When H_2O is codeposited with CO_2 on a substrate cooled to 77 K, a heterogeneous mixture of ASW and dry ice can form.[34] By subsequent high-pressure treatment, a so-called filled ice structure was produced[35-37] which, in fact, appears to display a chiral, the so-called S_χ framework structure.[38] It features open spiral channels along which the CO_2 guest molecules can move.

To examine the structure of amorphous and crystalline ices as well as possible phase changes in these materials, diffraction techniques and calorimetric methods are in widespread use. Conversely, relatively few experimental approaches are available that directly sense the slow water dynamics in the crystalline and amorphous ices. Among them are techniques such as nuclear magnetic resonance[39] and, as employed in the present work, dielectric relaxation spectroscopy. A very useful review of dielectric work on crystalline and amorphous ices covering work up to 2007 is available.[40] Previous dielectric studies concerned with the dynamics of HGW or ASW were either conducted as a function of temperature at a few frequencies,[9-11,41] or the samples were studied after pore collapse (with information on impurities trapped from the background gas between resulting lamellae or in remaining micropores not available).[42,43]

Effects of doping on the dynamics of amorphous[16,44-46] and crystalline[47-49] ices were also intensively examined. From dielectric as well as from calorimetric work, it has become clear that the implantation of defects into the H_2O network can make a distinctive difference. This is because doping with HCl and various other agents creates ice-typical ionic and/or Bjerrum defects that can lead to major changes in kinetic behavior when comparing crystalline with amorphous ices. For the crystalline ices these dopants, even when added in minute amounts ($<10^{-3}$ mole fraction), can enhance the hydrogen dynamics tremendously, sometimes by several orders of magnitude[47,50-52] thereby, e.g., being at the core of enabling phase transitions in various crystalline ices.[48,49] Conversely, for the numerous dopants tested so far, such enhancements appear to be absent in the amorphous ices.[16,44-46]

In order to explore the extent to which various *undoped* ice forms can be distinguished on the basis of dynamical properties, here we report on broadband dielectric spectra for HGW and compare them with dielectric results obtained for the amorphous ices ASW,[11,42,43] LDA, and HDA.[53] Further comparison is made with dielectric data reported for various *crystalline* ices, again, without

intentional impurity doping. While numerous results are available for ices studied under high pressure,[40] here we focus on ambient-pressure data for hexagonal ice[54-60] and phases that were prepared under high-pressure conditions.

The present compilation includes previously published results for ice V[51] and ice XII,[50] as well as data on the ices IV, VI, and the CO_2-filled S_χ clathrate hydrate. In the present context, it is important to realize that OCO is a linear and symmetric moiety so that it lacks a molecular dipole moment. Hence, dielectric measurements are not directly sensitive to its reorientational dynamics but to that of the H_2O molecules on their chiral framework structure.

II. EXPERIMENTAL DETAILS

The CO_2-filled S_χ clathrate hydrate was obtained as described previously in Ref. 37. In brief, 0.02 mbar of CO_2 and 0.20 mbar of H_2O vapor were first co-deposited for 12 h on a copper plate kept at 77 K in a high-vacuum chamber, thus forming millimeter thick layers of amorphous solid water containing CO_2-filled micropores mixed with crystalline CO_2 (dry ice). The recovered deposit was then transferred at 77 K and ambient pressure to a high-pressure cell, in which it was compressed to 1.8 GPa and heated to 250 K. This produces a mixture of dry ice and ice VI, which subsequently is decompressed at 250 K to 0.60 GPa to form the S_χ clathrate hydrate, which is finally quenched to 77 K and ambient pressure. The X-ray diffractogram shows that the sample is composed of mainly the S_χ clathrate, with a few percent of unreacted dry ice and ice VI remaining (see Ref. 37).

The ice IV sample was prepared as described in Ref. 61. In brief, pure (undoped) hexagonal ice was first amorphized in the high-pressure cell by compression at 77 K to 1.6 GPa and then heated at 0.81 GPa to ~170 K. We used a low heating rate of 0.4 K/min to avoid parallel crystallization of ice XII. The X-ray diffractogram shows pure ice IV, with a contamination of 1%–3% of ice XII.

The pure (undoped) ice VI sample was prepared as described in Ref. 62. In brief, 600 μl of pure water were frozen to hexagonal ice at 77 K, compressed to 1.0 GPa, and heated to 250 K (at 20–25 K/min). Upon heating, amorphization, crystallization to ice XII, and finally the polymorphic transition to ice VI are observed. Then, the sample is quenched (at about 100 K/min) and recovered at ambient pressure. The X-ray diffractogram shows pure ice VI, without any by-phase beyond the noise level.

HGW was prepared as described in Ref. 63. In brief, an aerosol containing water droplets of about 5 μm in diameter was generated using an ultrasonic nebulizer and introduced through a 300 μm orifice into a high-vacuum chamber containing a cold-finger equipped with a cooper plate kept at ~80 K. The impact of the droplets at ultrasonic speed results in splat cooling rates of 10^6–10^7 K/s, thereby avoiding crystallization. The deposition was maintained for about half an hour, after which the cold finger was removed from the vacuum chamber and immersed in liquid nitrogen. X-ray diffraction shows the powder scratched from the copper plate to be pure HGW, with contamination by ice I on the order of 1%. After scratching the deposit off from the cold plate onto which it was condensed, the resulting fine powder was transferred to Dortmund and used to fill an invar/sapphire parallel-plate capacitor at liquid nitrogen temperatures according to procedures described elsewhere.[53]

All dielectric measurements reported in the present work were carried out at ambient pressure using an Alpha analyzer in conjunction with a Quatro temperature controller from Novocontrol. Prior to the acquisition of each spectrum, the temperature was stabilized within a deviation range of ±0.1 K. For the representation of the dielectric relaxation, we adhere to our previous convention that time scales directly obtained from a loss peak are shown as filled symbols while open symbols represent data for which time-temperature superposition (TTS)[64] was exploited.

III. EXPERIMENTAL RESULTS

A. Hyperquenched glassy water

After filling the capacitor under liquid nitrogen conditions, the HGW powder sample was heated with an average of about 2.8 K/h. The frequency dependent dielectric loss ε'' obtained for HGW is depicted in Fig. 1. At 110 K, a (somewhat noisy) high-frequency wing of a loss feature as well as a separated rather broad low-amplitude peak (with a local maximum near 100 Hz) appears. Upon heating, the wing feature moves through the measurement window toward higher frequencies and develops itself into a flank of a dominant relaxation peak. At 134 and 137 K, where additional low-frequency (<0.01 Hz) measurements are carried out, not only the flank but also the maximum of the main peak could be resolved.

The shape of the main process seems to change very slightly with temperature. Assuming that the (not always determined) peak amplitude is more or less constant, the steepness of the high-frequency flank slightly increases with temperature suggesting that the peak width narrows somewhat upon heating. The small peak (appearing near 100 Hz at 110 K) is less sensitive to temperature changes. Hence, toward higher temperatures, it becomes increasingly difficult to resolve it reliably from the main process.

From the more abrupt change of the spectral shape observed upon further temperature increase (see the red dots and the dashed line in Fig. 1), 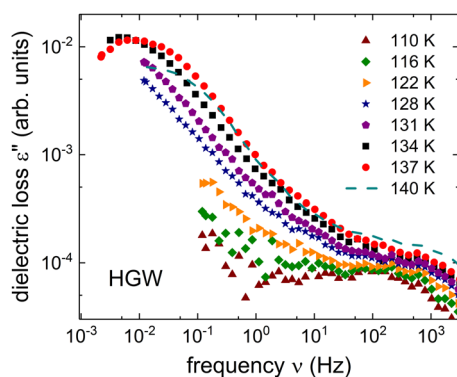one infers that our HGW sample crystallizes to stacking-disordered ice between 137 and 140 K. These temperatures are significantly lower than the about 150 K which were reported for the crystallization transition of LDA[53] as well as for that of ASW after pore collapse.[42] Thus, our HGW specimen seems to be kinetically rather unstable. Similar observations were made in calorimetric studies,[63] in which it was inferred that the small amounts of crystallized material (see Sec. II) act as seeds for ice growth upon heating.

B. CO₂-filled Sχ clathrate hydrate

The CO_2-filled clathrate hydrate, in a first run, was heated with an average rate of about 3.9 K/h from 96 to 129 K, and measurements were taken in steps of 3 K. The corresponding dielectric loss curves, shown in Fig. 2(a), look surprisingly similar to those for HGW. In particular, one recognizes, again, a two-peak structure. The high-frequency feature appears spectrally somewhat less separated than for HGW.

After thermally annealing the sample for 140 min at 129 K, it was cooled back to 114 K within about 15 min. Then, a second heating run with an average rate of 4.2 K/h was started that yielded the results shown in Fig. 2(b). From a close inspection, it is found that the shape of the main contribution to the dielectric loss is practically temperature independent so that TTS applies well. Thus, overall, the loss curves display a smooth evolution up to temperatures of 144 K.
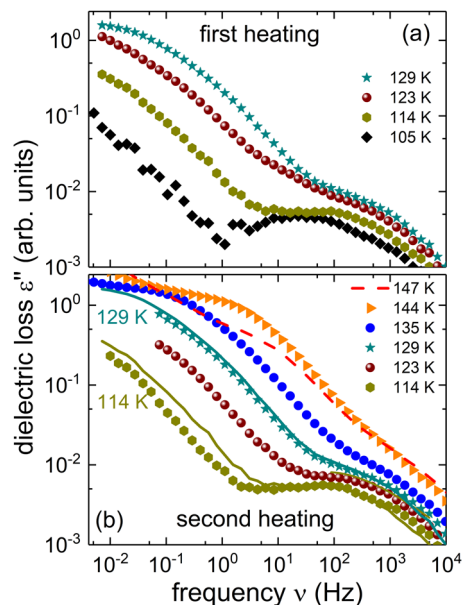
FIG. 2. Dielectric loss spectra obtained during (a) the first and (b) the second heating run performed for CO_2-filled S_χ clathrate hydrate. For comparison, in panel (b), two spectra from the first heating run are included as solid lines. At 129 K, the spectra superimpose well, while at 114 K, differences are seen in the region of the main peak. The decomposition of the S_χ clathrate to CO_2 and hexagonal ice[37] leads to significant changes of the low-frequency part of the spectral shape, while its high-frequency part remains practically unchanged. Data recorded at 147 K which indicate a qualitative change within the sample are represented as a dashed line.

FIG. 1. Dielectric loss spectra of HGW as measured at several temperatures are represented as symbols. Data corresponding to measurements in the stacking disordered crystalline phase are represented as a dashed line.

In this temperature range (100–140 K), the slow decomposition of the S_χ phase takes places, while CO_2 is expelled and the clathrate lattice transforms to hexagonal ice.[37]

Then, at 147 K, the loss behavior has changed in a qualitative fashion; see Fig. 2(b). In Ref. 37, the transition of the by-phase ice VI to stacking disordered cubic ice was reported to occur near this temperature from calorimetric and X-ray diffraction experiments employing rates of 3 K/min.

At first glance, the two data sets obtained for the CO_2-filled clathrate hydrate look relatively similar. In order to demonstrate that indeed only small differences can be recognized, in Fig. 2(b), we include the dielectric losses from the initial run for 114 and 129 K as solid lines. For the higher temperature, the spectra essentially coincide with respect to the low-frequency as well as with respect to the high-frequency contributions. Conversely, at the lower temperature, significant differences regarding the low-frequency portion of the spectra show up. Obviously, the annealing of the sample, which occurred between the two measurements recorded at 114 K, has led to an irreversible change. This effect manifests itself in a down-shift of the spectrum along the frequency axis by about 0.3 decades, while the high-frequency feature is essentially unaltered. As noted above, this irreversible change has been attributed to the slow release of gaseous CO_2 from the clathrate in the temperature range from 100 to 140 K, converting parts of the clathrate lattice gradually to hexagonal ice.[37]

Like the presently studied CO_2-filled clathrate hydrate, also ASW is produced by vapor deposition which yields a microporous solid. For ASW, it was reported that on its pore surface, a small number of "dangling" water molecules or OH groups can exist that perform a reorientational motion which is much faster than the dipole motion in the bulk.[9] These dynamics lead to a weak, barely thermally activated high-frequency peak that does not occur in sintered[65] ASW or in HGW.[66] At present, it is not known whether the micropores still present in ASW after pore collapse[31] are removed completely using the temperature/pressure protocol that is required to produce the CO_2-filled clathrate hydrate.

C. Crystalline ices

In Fig. 3, we compile ambient-pressure dielectric loss spectra for the crystalline ice phases I_h (hexagonal ice),[67] IV, and VI (all measured in the course of this work) as well as for ice V[51] and ice XII.[50] These (and other nominally pure) crystalline ices are well known to display orientational glass transitions.[46,68–70] During such a transition, the hydrogen degrees of freedom freeze upon cooling, giving rise to a calorimetrically detectable signature, while the crystalline center-of-mass lattice remains unaffected. In dielectric spectroscopy, the freezing transition of the crystalline ices is typically accompanied by a thermally activated slow-down of the dipolar degrees of freedom.

From Fig. 3, it is obvious that (except for some of the smallest losses shown) a rather well-defined high-frequency power law $\varepsilon'' \propto \nu^{-\alpha}$ is found. Here, an inverse proportionality, $\varepsilon'' \propto \nu^{-1}$, corresponds to a Debye-type of spectral shape. In fact, such a power law is closely followed by the loss spectrum of ice I_h that is included in Fig. 3(a). Also for the other crystalline ices, the power-law exponent α is always ≥ 0.8, thus indicating a relaxation that is rather close to an exponential process.
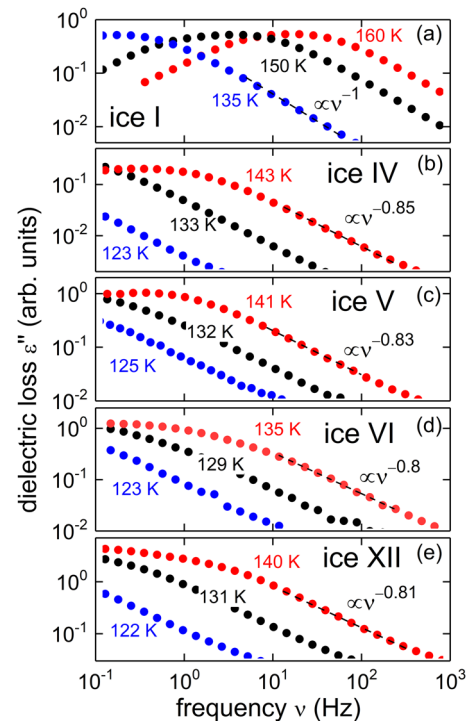

FIG. 3. Dielectric loss spectra of the crystalline ice phases (a) I_h (present work), (b) IV (present work), (c) V,[51] (d) VI (present work), and (e) XII.[50] The dashed lines refer to power laws $\varepsilon'' \propto \nu^{-\alpha}$ as indicated.

Interestingly, not only the shapes but also the time scales at least of the ices V and XII are very similar, while the dynamics in ice VI (and the present ice I_h sample) is somewhat faster and the dynamics in ice IV is slightly slower. These findings agree with the orientational glass transition temperature of ice VI ($\approx$128 K) being slightly lower than the ones of ice V and ice XII ($\approx$131 K); see Table II in Ref. 46. However, based on its calorimetric orientational glass transition temperature ($\approx$140 K), the time scale for ice IV would be expected to be significantly longer than for all other high-pressure crystalline ices compiled in Ref. 46.

IV. DISCUSSION

The availability of frequency and temperature dependent dielectric losses for a number of crystalline and amorphous ices calls for their detailed comparison with the goal to shed light on issues such as:

i. Can the various amorphous ice forms be distinguished on the basis of the spectral shapes of their dominant low-frequency loss contribution?

ii. Does this shape provide a means to distinguish amorphous from crystalline ices?

iii. Do the mean time scales of the various low-density amorphous ice forms display a similar behavior or not?

iv. How do the time scales of the amorphous ices compare with those of the crystalline ones?

To start addressing these questions, in Fig. 4(a), we summarize the dielectric loss spectra of several amorphous ices and compare them with various other systems. For the sake of a better comparability, the spectra are all scaled to the same peak amplitude and to the same peak frequency.

With item (i) in mind and focusing on the high-frequency flank of the peak, one recognizes some diversity of behavior. As noted earlier,[53] the spectral shape of HDA closely resembles that of glycerol, a prototypical "type A" glass former.[71] Such liquids feature a near-peak slope of $\varepsilon'' \propto \nu^{-\alpha}$ with an exponent close to 0.5. At higher frequencies, this approximate power-law region is followed by a more curved behavior, the so-called excess wing. The VHDA data that were measured at a pressure of 1 GPa indicate an exponent slightly larger than 0.5. However, from those data that were digitized from Ref. 15, it is unclear whether or not an excess wing might be present in that sample; see Fig. 4(a).

A curved $\varepsilon''(\nu)$ behavior can also be discerned for HGW, while for LDA, a power-law behavior is followed for frequencies extending up to more than 2 decades above the peak region. Then, hints for an additional excitation show up for LDA. With reference to earlier work,[9,11] this feature was speculated to be linked to a so-called Johari-Goldstein β-relaxation.[53] Glass formers displaying these kinds of localized motions were previously classified as being of "type B."[71] For the ASW sample that had undergone pore collapse, such a feature appears to be absent:[42] its dielectric loss
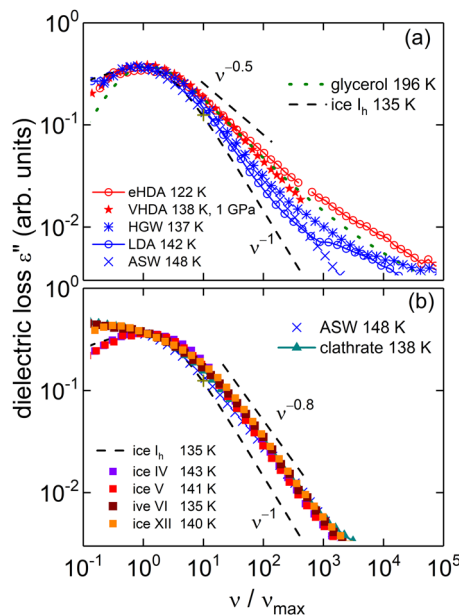
follows a high-frequency power law with an exponent $\alpha \approx 0.75$. Thus, from Fig. 4(a), it is clear that all amorphous ices display a non-Debye-like spectral shape.

To addresses item (ii), which concerns potential shape differences between crystalline and amorphous ices, Fig. 4(b) summarizes dielectric losses acquired for several crystalline ices after normalization with respect to frequency and amplitude. For the high-pressure-generated ices, the high-frequency flank of $\varepsilon''(\nu)$ is almost coincident with that of ASW and the CO_2-filled clathrate hydrate. Near and below the peak region, the data for the latter as well as for the ice VI sample seem to be overlaid by additional effects.

A whole zoo of orientational glasses or supercooled plastic phases (not involving H_2O) is known, for an overview on dielectric results of such systems; see, e.g., Ref. 72. Many "glassy crystals" like *ortho*- and *meta*-carborane do not show a high-frequency wing, while some others like cyclohexanol and pentachloronitrobenzene do. For supercooled liquids, the emergence of a high-frequency power law devoid of a wing seems to be the exception rather than the rule.[73] Hence, the spectral shape of HDA, LDA, and HGW is more akin to that of viscous liquids than to that of supercooled plastic crystals.

At first sight, the compilation of dielectric spectra in Fig. 4 suggests that the slope and curvature of the high-frequency losses provides a means to distinguish crystalline form amorphous ices. However, a closer scrutiny reveals that such a simple criterion may not be appropriate. Particularly startling is the case of the CO_2-filled clathrate hydrate. The shape and overall appearance of its dielectric loss spectra are strikingly similar to those of HGW, including the peaked high-frequency feature. Thus, one is misleadingly tempted to conclude that the two systems might be very closely related. As will be discussed near the end of the present Sec. IV, it is well possible that the microscopic origin of the high-frequency peaks of the clathrate hydrate and of HGW is quite different. Nevertheless, in view of the various (phenomenologically apparent) exceptions on both sides, we have to state that the present observations concerning the spectral shapes do not provide clear-cut criteria that would allow one to decide upon the nature of the glassy state in the amorphous ices.

Let us now discuss item (iii), i.e., the time scales of the amorphous ices as measured by dielectric spectroscopy above their glass transition temperature. As noted above, the time scales obtained at ambient pressure from peak frequencies (full symbols) or from TTS[64] (open symbols) are compiled in Fig. 5(a). One recognizes that the dipolar relaxation times for HDA are shortest and that those of LDA and HGW are relatively similar to each other and close to the time scale determined for ASW in Ref. 10. Remarkably, the time scales from ASW as reported in Refs. 42 and 43 are significantly longer. The difference in relaxation time of the latter data and those of LDA was noted and rationalized in Ref. 42 with reference to the fluffy, high-surface-area nature of the vapor deposit, and the possibility of (unspecified) impurities taken up from the background gas in its highly microporous form before pore collapse. In fact, the main difference between ASW and LDA (or HGW) samples is the high surface area and the porosity of the former amorphous ice. At 77 K, the surface area of ASW is typically a few hundred times larger than for LDA or HGW. In the astrophysical literature (e.g., Ref. 33), such high-surface-area samples are often called porous ASW (p-ASW) and they are prone to an uncontrolled uptake of background gas

FIG. 4. (a) Dielectric loss spectra of HDA,[53] LDA,[53] HGW (this work), VHDA[15] (measured at a pressure of 1 GPa), as well as ASW that underwent pore collapse.[42,43] All data are presented after normalizing them with respect to amplitude and peak frequency. For comparison, spectra for glycerol (from Ref. 71) and hexagonal ice (present work) are included. The dashed lines refer to power laws $\varepsilon'' \propto \nu^{-\alpha}$ as indicated. For comparison, frame (b) shows dielectric loss spectra for the crystalline ices IV, V,[51] VI, and XII[50] as well as for CO_2-filled clathrate hydrate. Note that a peak maximum cannot be identified clearly for the data of ice VI and of the CO_2-filled clathrate hydrate.
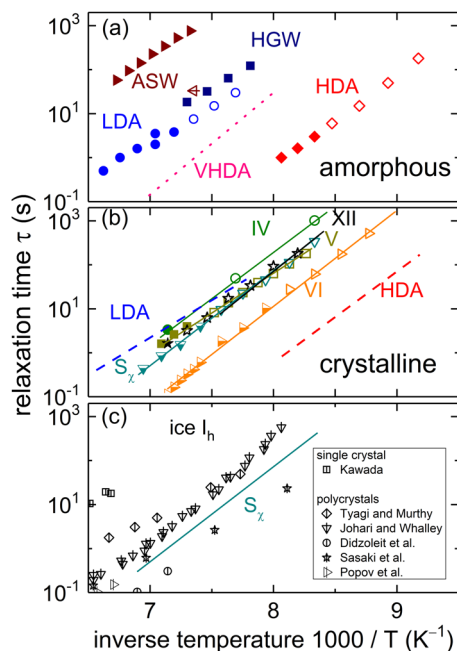
FIG. 5. (a) Dielectric relaxation times of the amorphous ices HDA,[53] LDA,[53] HGW (this work), and ASW after pore collapse[42,43] are represented as open and solid symbols. The barred triangle refers to annealed ASW and is a result taken from Ref. 10. For comparison, the relaxation times of the pure high-density samples from Ref. 16 (here called VHDA) are represented as dotted line. The corresponding measurements were carried out at 1 GPa. By contrast, all other data represented in this plot refer to ambient-pressure experiments. (b) The relaxation times of the crystalline ices IV, V,[51] VI, and XII[50] are represented as symbols, those of LDA and HDA as dashed lines. The half-filled points for the CO_2-filled clathrate hydrate and for ice VI were obtained by matching the high-frequency flank of their main process to that of the HGW sample. The solid lines guide the eye. (c) Data for hexagonal ice as compiled from work by Kawada,[55] Johari and Whalley,[56] Tyagi and Murthy,[57] Didzoleit et al.,[58] Sasaki et al.,[59] and Popov et al.[60] For comparison, we include the line from frame (b) which represents the data of the CO_2-filled S_χ clathrate hydrate.

even under high-vacuum conditions. At about 120–140 K, a pore collapse process takes place, leading to what is termed compact ASW (c-ASW) in the astrophysical nomenclature. Even though the pore collapse reduces the surface area by two orders of magnitude, a 2D lamellar structure with some trapped micropores remains.[31,32] In other words, c-ASW is in fact still not free from interfaces and pores. The most likely reason for the difference in the relaxation time between ASW and LDA/HGW are these interfaces and pores, and possibly impurities that might be trapped within them. Currently, it is not known whether these features are also leading to the somewhat exceptional high-frequency wing of c-ASW after pore collapse, a sample which does not display curvature on the double logarithmic plot, cf. Fig. 4(a), the way the other amorphous ices do.

To compare the time scales of the amorphous ices with those of the crystalline ones, cf. item (iv), Fig. 5(b) summarizes the dipolar relaxation times of the ices IV, V,[51] VI, XII,[50] and the CO_2-filled clathrate hydrate. One recognizes that the time scales for most of the

high-pressure-produced ices and the S_χ clathrate are relatively close to each other and near those of LDA. Then, in Fig. 5(c), we summarize data for single- and poly-crystalline hexagonal ice from various sources.[55–60] Depending on the preparation route and presumably also affected by the number of unintentionally implemented impurities, at a given temperature, the time scale of this ice phase strongly varies. Yet, the most extensive data set for the relaxation times in that figure, reported by Johari and Whalley,[56] is again close to that of LDA. However, these data show a significantly curved behavior, which seems to distinguish them from the other relaxation times in the shown temperature range.

At first glance, the similarity of the time scales of the crystalline with those of the amorphous ices as well as the similarity of the differential scanning calorimetry (DSC) signals of, e.g., LDA and ice XII,[69] is not incompatible with an orientational glass scenario for the amorphous ices. Hence, from corresponding measurements of the dynamics in *pure* ices alone, it is hard to conclude reliably on the detailed nature of the underlying glass transition scenarios.

From the data summarized in Fig. 5(b), it becomes clear that density does not play the role one may have naïvely expected. Larger mass densities do not simply generate an enhanced motional hindering and thus slowdown of the reorientational dynamics. On the one hand, it is well documented that HDA is about 20%–25% denser than LDA, yet it relaxes faster than the less dense LDA. On the other hand,[74] ice IV despite being about 38% denser displays time scales similar to those of LDA. Furthermore, while ice VI is only 3% denser than ice IV, it relaxes much faster than LDA.

It is clear that factors other than density are affecting the time scale of the ices, such as, for instance, the O–O distance. The—on average—fivefold coordination of H_2O in HDA, occasionally referred to as interstitial water molecule, increases the O–O distance in HDA by ~2% with respect to that in LDA.[14] This "density–distance paradox" was suggested to rationalize the slower relaxation in HDA.[53] Conversely, if the relaxation in the amorphous ices was dominated by effects of proton transfer in a double well, an enhanced separation between the well should lead to slower dynamics. Reasonably assuming that the separation of the wells increases with the O–O distance, a prevalence of proton transfer processes would predict that the relaxation in HDA is slower than in LDA, at variance with the experimental findings. This suggests that the dielectric relaxation in amorphous ices is governed by a mechanism different from just proton hopping.

With the goal to distinguish between different glass transition scenarios, also isotope substitution experiments were carried out.[4,42,43,46] As put forward in the Introduction, to resolve the issue by means of low-frequency experiments, in our view an important piece of evidence comes from investigations using (ionic) doping via suitable acids or bases.

By employing a nonionic and even nonpolar additive such as CO_2 a significant alteration of the water dynamics appears unlikely, in any case. Indeed, as Fig. 5(a) suggests, a major direct impact of bulklike carbon dioxide on the H_2O reorientation dynamics of our filled sample cannot be discerned. In this context, it is interesting to note that from nuclear magnetic resonance[75] and dielectric experiments,[76] the dynamics of crystalline CO_2 is known to take place on the submillihertz scale when extrapolated to temperatures near 150 K. The high-frequency dielectric constant of CO_2 is estimated[76] to be about 1.7. Thus, the dielectric contrast between CO_2 and water

(with its large dielectric constant) is comparable to that of unfilled pore space and water.

For ASW, the effect of removing pore space by sintering has an impact on the high-frequency contribution to the dielectric loss; this has been discussed in relation to the Johari-Goldstein secondary relaxation.[9]

Whether the high-frequency peaks seen for HGW in Fig. 1 refer to such a relaxation cannot be decided on the basis of the present data. It is clear, however, that the temperature dependence of these peak frequencies is much weaker than expected for such a secondary process.[77] Hence, it is worthwhile to apply other experimental techniques that are sensitive to the molecular dynamics such as nuclear magnetic resonance which has been useful to unravel details of Johari-Goldstein relaxations in typical (nonaqueous) glass formers.[78] For the CO_2-filled S_χ clathrate hydrate, the origin of the high-frequency contribution to the dielectric loss, see Fig. 2, is particularly cumbersome. Secondary relaxations are observed for many glass forming materials, but they are not a feature expected to occur in clathrate hydrates. The possibility of contributions from "dangling" water molecules and OH groups was already mentioned in Sec. III B. Hints regarding a further possible origin of the high-frequency contribution, presently detected in the CO_2-filled clathrate hydrate, can be gained from work on cubic structure I and II clathrate hydrates:[79,80] Studies with a focus on the kinetics of the water molecules typically reveal a single loss peak behavior, irrespective of the chosen guest molecules. Similar observations were made for a pressure-collapsed clathrate hydrate (THF·16.65H_2O) containing tetrahydrofuran (THF) guests.[81] These samples, with relaxation times comparable to those of HDA, also yield a spectrum characteristic of a homogeneous one-phase sample.[81] This behavior prevails until a partial transformation to another state sets in upon heating,[81] eventually leading to the emergence of a two-component spectrum.[82] As mentioned near the end of Sec. III B, a two-phase mixture is indeed expected to occur for the presently studied CO_2-filled S_χ clathrate hydrate which thus may rationalize the appearance of the high-frequency feature.

For further comparison and to shed light on the surprising dynamical behavior of the CO_2-filled clathrate hydrate, it should be helpful to scrutinize also its amorphous precursor with and without small-molecule filling.

V. SUMMARY

To summarize, we presented dielectric loss data for HGW and compared its spectral shape with that of the other amorphous ice forms LDA and HDA. On the high-frequency side of their loss peaks, we found a curved behavior, except for a previously studied[43] c-ASW[42] sample that had undergone pore collapse. Measurements were carried out also for several crystals (ice IV, ice VI, and a CO_2-filled clathrate hydrate) as well and compared with published results for ice V and XII. To a good approximation, all of these samples display high-frequency power laws $\varepsilon'' \propto \nu^{-\alpha}$ with slopes $\alpha \geq 0.8$, except for the CO_2-filled clathrate hydrate for which a high-frequency feature (in the 10^2–10^3 Hz range) becomes visible at lower temperatures. The overall behavior of this sample strongly resembles that of HGW and highlights some of the difficulties encountered when trying to distinguish amorphous from crystalline ices based on dielectric results alone.

Also the observation that the relaxation times of the undoped ices are rather close to each other hampers a clear distinction of amorphous from crystalline ices. In the presently accessible temperature range, the dipolar time scales in ice IV, V, XII, the CO_2-filled clathrate hydrate, and LDA differ by less than a factor of five, while ice VI and, in particular, HDA display significantly faster dynamics.

Thus, with respect to the four questions raised in Sec. IV, we found

(i) There is a trend that the responses of the more highly dense amorphous ices (VHDA, HDA) are slightly broader (indicating an enhanced dynamic heterogeneity) than those of the low-density amorphous ices (LDA, HGW, compact ASW). Despite this trend, one has to recognize that the differences in the widths of the various ice states are not very pronounced. Therefore, one obviously cannot clearly distinguish the various amorphous ice forms based on the spectral shapes of their dominant low-frequency loss contributions.

(ii) All of the amorphous ices (except ASW after pore collapse) for which frequency spectra are available display a rather curved high-frequency wing, while the high-frequency flank of the studied crystalline high-pressure-produced ice phases (not including the CO_2-filled clathrate hydrate) display an approximate power law. Thus, disregarding the data of ASW that has undergone pore collapse,[42,43] the peak shape provides some hints as to whether one deals with a nominally pure amorphous ice or a nominally pure crystalline ice.

(iii) Again with the exception of the data for ASW after pore collapse, but including other data on (nominally pure) ASW,[9] at a given temperature, the time scales of the various low-density amorphous ice forms display very similar values. Furthermore, referring to item (i), the similar behavior of (nominally pure) ASW, HGW, and LDA clearly distinguishes them from the high-pressure variants (VHDA, HDA).

The exceptional behavior of the ASW sample after pore collapse[43] with respect to the time scale as well as to the spectral shape corroborates the previous inference that this sample may indeed be affected by trapping of (unspecified) background gases within micropores or at the interfaces between lamellae. Therefore, further measurements of ASW deposited at higher temperatures, avoiding the need for the pore collapse, are warranted that pursue the goal to map out its dielectric loss spectrum.

(iv) The relaxation times of the crystalline ices are of a magnitude that is in between those of HDA and LDA, at least in the time scale range between about 0.1 and 100–1000 s where information is currently available. Hence, the amorphicity of the ice structure does not appear to have a distinctive impact on the measured time scales. The way that density may affect the relaxation is not obvious as well, calling for further study also of this aspect of the relaxation dynamics of the amorphous ices.

Thus, dielectric relaxation spectroscopy alone yields, at best, circumstantial evidence regarding the nature of the dynamic freezing that is taking place in nominally pure amorphous and crystalline ices.

The situation is different in the presence of ionic doping as provided by suitable acids, bases, or salts. It has been shown previously that, while suitable dopants have an appreciable bearing on the dipolar dynamics of the crystalline ices,[47,50–52] for the amorphous ices,[3,45,46] the impact of doping is practically negligible.

REFERENCES

[1]C. A. Angell, "Amorphous water," Annu. Rev. Phys. Chem. **55**, 559 (2004); "Insights into phases of liquid water from study of its unusual glass-forming properties," Science **319**, 582 (2008).

[2]S. Capaccioli and K. L. Ngai, "Resolving the controversy on the glass transition temperature of water?," J. Chem. Phys. **135**, 104504 (2011).

[3]K. Amann-Winkel, R. Böhmer, C. Gainaru, F. Fujara, B. Geil, and T. Loerting, "*Colloquium*: Water's controversial glass transitions," Rev. Mod. Phys. **88**, 011002 (2016).

[4]J. J. Shephard and C. G. Salzmann, "Molecular reorientation dynamics govern the glass transitions of the amorphous ices," J. Phys. Chem. Lett. **7**, 2281 (2016).

[5]F. Perakis *et al.*, "Diffusive dynamics during the high-to-low density transition in amorphous ice," Proc. Natl. Acad. Sci. U. S. A. **114**, 8193 (2017).

[6]E. F. Burton and W. F. Oliver, "X-ray diffraction patterns of ice," Nature **135**, 505 (1935).

[7]P. Brüggeller and E. Mayer, "Complete vitrification in pure liquid water and dilute aqueous solutions," Nature **288**, 569 (1980); E. Mayer, "New method for vitrifying water and other liquids by rapid cooling of their aerosols," J. Appl. Phys. **58**, 663 (1985).

[8]J. H. E. Cartwright, B. Escribano, and C. I. Sainz-Diaz, "The mesoscale morphologies of ice films: Porous and biomorphic forms of ice under astrophysical conditions," Astrophys. J. **687**, 1406 (2008).

[9]G. P. Johari, A. Hallbrucker, and E. Mayer, "The dielectric behavior of vapor-deposited amorphous solid water and of its crystalline form," J. Chem. Phys. **95**, 2955 (1991).

[10]G. P. Johari, "State of water at 136 K determined by its relaxation time," Phys. Chem. Chem. Phys. **7**, 1091 (2005).

[11]G. P. Johari, A. Hallbrucker, and E. Mayer, "Dielectric study of the structure of hyperquenched glassy water and its crystallized forms," J. Chem. Phys. **97**, 5851 (1992).

[12]O. Mishima, L. D. Calvert, and E. Whalley, "An apparently first-order transition between two amorphous phases of ice induced by pressure," Nature **314**, 76 (1985).

[13]O. Mishima, L. D. Calvert, and E. Whalley, "'Melting ice' I at 77 K and 10 kbar: A new method of making amorphous solids," Nature **310**, 393 (1984).

[14]T. Loerting, C. Salzmann, I. Kohl, E. Mayer, and A. Hallbrucker, "A second distinct structural state of high-density amorphous ice at 77 K and 1 bar," Phys. Chem. Chem. Phys. **3**, 5355 (2001).

[15]O. Andersson, "Relaxation time of water's high-density amorphous ice phase," Phys. Rev. Lett. **95**, 205503 (2005).

[16]O. Andersson and A. Inaba, "Dielectric properties of high-density amorphous ice under pressure," Phys. Rev. B **74**, 184201 (2006).

[17]O. Andersson, "Dielectric relaxation of the amorphous ices," J. Phys.: Condens. Matter **20**, 244115 (2008).

[18]T. Loerting, K. Winkel, M. Seidl, M. Bauer, C. Mitterdorfer, P. H. Handle, C. G. Salzmann, E. Mayer, J. L. Finney, and D. T. Bowron, "How many amorphous ices are there?," Phys. Chem. Chem. Phys. **13**, 8783 (2011).

[19]M. M. Koza, T. Hansen, R. P. May, and H. Schober, "Link between the diversity, heterogeneity and kinetic properties of amorphous ice structures," J. Non-Cryst. Solids **352**, 004988 (2006); P. Handle and T. Loerting, "Dynamics anomaly in high-density amorphous ice between 0.7 and 1.1 GPa," Phys. Rev. B **93**, 064204 (2016);

"Experimental study of the polyamorphism of water. II. The isobaric transitions between HDA and VHDA at intermediate and high pressures," J. Chem. Phys. **148**, 124509 (2018) and references cited therein.

[20]J. J. Shephard, S. Ling, G. C. Sosso, A. Michaelides, B. Slater, and C. G. Salzmann, "Is high-density amorphous ice simply a 'derailed' state along the ice I to ice IV pathway?," J. Phys. Chem. Lett. **8**, 1645 (2017).

[21]C. A. Tulk, D. D. Klug, J. J. Molaison, A. M. dos Santos, and N. Pradhan, "Structure and stability of an amorphous water-methane mixture produced by cold compression of methane hydrate," Phys. Rev. B **86**, 054110 (2012).

[22]O. Andersson and U. Haussermann, "A second glass transition in pressure collapsed type II clathrate hydrates," J. Phys. Chem. B **122**, 4376 (2018) and references cited therein.

[23]A. Bizid, L. Bosio, A. Defrain, and M. Oumezzine, "Structure of high-density amorphous water. I. X-ray diffraction study," J. Chem. Phys. **87**, 2225 (1987).

[24]D. T. Bowron, J. L. Finney, A. Hallbrucker, I. Kohl, T. Loerting, E. Mayer, and A. K. Soper, "The local and intermediate range structures of the five amorphous ices at 80 K and ambient pressure: A Faber-Ziman and Bhatia-Thornton analysis," J. Chem. Phys. **125**, 194502 (2006); D. Mariedahl, F. Perakis, A. Späh, H. Pathak, K. H. Kim, G. Camisasca, D. Schlesinger, C. Benmore, L. G. M. Pettersson, A. Nilsson, and K. Amann-Winkel, "X-ray scattering and O–O pair-distribution functions of amorphous ices," J. Phys. Chem. B **122**, 7616 (2019).

[25]Y. P. Handa and D. D. Klug, "Heat capacity and glass transition behavior of amorphous ice," J. Chem. Phys. **92**, 3323 (1988).

[26]G. P. Johari, A. Hallbrucker, and E. Mayer, "The glass–liquid transition of hyperquenched water," Nature **330**, 552 (1987).

[27]A. Hallbrucker, E. Mayer, and G. P. Johari, "Glass–liquid transition and the enthalpy of devitrification of annealed vapor-deposited amorphous solid water. A comparison with hyperquenched glassy water," J. Phys. Chem. **93**, 4986 (1989).

[28]A. Hallbrucker, E. Mayer, and G. P. Johari, "The heat capacity and glass transition of hyperquenched glassy water," Philos. Mag. B **60**, 179 (1989).

[29]E. Mayer, "Calorimetric glass transitions in the amorphous forms of water: A comparison," J. Mol. Struct. **250**, 403 (1991).

[30]M. S. Elsaesser, K. Winkel, E. Mayer, and T. Loerting, "Reversibility and isotope effect of the calorimetric glass → liquid transition of low-density amorphous ice," Phys. Chem. Chem. Phys. **12**, 708 (2010).

[31]C. R. Hill, C. Mitterdorfer, T. G. A. Youngs, D. T. Bowron, H. J. Fraser, and T. Loerting, "Neutron scattering analysis of water's glass transition and micropore collapse in amorphous solid water," Phys. Rev. Lett. **116**, 215501 (2016).

[32]C. Mitterdorfer, M. Bauer, T. G. A. Youngs, D. T. Bowron, C. R. Hill, H. J. Fraser, J. L. Finney, and T. Loerting, "Small-angle neutron scattering study of micropore collapse in amorphous solid water," Phys. Chem. Chem. Phys. **16**, 16013 (2014).

[33]R. A. Baragiola, "Microporous amorphous water ice thin films: Properties and their astronomical implications," in *Water in Confining Geometries*, edited by V. Buch and J. P. Devlin (Springer-Verlag, Heidelberg, 2003).

[34]C. Mitterdorfer, M. Bauer, and T. Loerting, "Clathrate hydrate formation after CO_2–H_2O vapour deposition," Phys. Chem. Chem. Phys. **13**, 19765 (2011).

[35]H. Hirai, K. Komatsu, M. Honda, T. Kawamura, Y. Yamamoto, and T. Yagi, "Phase changes of CO_2 hydrate under high pressure and low temperature," J. Chem. Phys. **133**, 124511 (2010).

[36]O. Bollengier, M. Choukroun, O. Grasset, E. Le Menn, G. Bellino, Y. Morizet, L. Bezacier, A. Oancea, C. Taffin, and G. Tobie, "Phase equilibria in the H_2O–CO_2 system between 250–330 K and 0–1.7 GPa: Stability of the CO_2 hydrates and H_2O-ice VI at CO_2 saturation," Geochim. Cosmochim. Acta **119**, 322 (2013).

[37]B. Massani, C. Mitterdorfer, and T. Loerting, "Formation and decomposition of CO_2-filled ice," J. Chem. Phys. **147**, 134503 (2017).

[38]D. M. Amos, M.-E. Donnelly, P. Teeratchanan, C. L. Bull, A. Falenty, W. F. Kuhs, A. Hermann, and J. S. Loveday, "A chiral gas-hydrate structure common to the carbon dioxide-water and hydrogen-water systems," J. Phys. Chem. Lett. **8**, 4295 (2017).

[39]F. Löw, K. Amann-Winkel, T. Loerting, F. Fujara, and B. Geil, "Ultra-slow dynamics in low density amorphous ice revealed by deuteron NMR: Indications for a glass transition," Phys. Chem. Chem. Phys. **15**, 9308 (2013) and references cited therein.

[40]G. P. Johari and O. Andersson, "Vibrational and relaxational properties of crystalline and amorphous ices," Thermochim. Acta **461**, 14 (2007) and references cited therein.

[41]V. P. Koverda, N. M. Bogdanov, and V. P. Skripov, "Self-sustaining crystallization of amorphous layers of water and heavy water," J. Non-Cryst. Solids **57**, 203 (1983).

[42]C. Gainaru, A. L. Agapov, V. Fuentes-Landete, K. Amann-Winkel, H. Nelson, K. W. Köster, A. I. Kolesnikov, V. N. Novikov, R. Richert, R. Böhmer, T. Loerting, and A. P. Sokolov, "Anomalously large isotope effect in the glass transition of water," Proc. Natl. Acad. Sci. U. S. A. **111**, 17402 (2014).

[43]A. L. Agapov, A. I. Kolesnikov, V. N. Novikov, R. Richert, and A. P. Sokolov, "Quantum effects in the dynamics of deeply supercooled water," Phys. Rev. E **91**, 022312 (2015).

[44]G. P. Johari, A. Hallbrucker, and E. Mayer, "Isotope and impurity effects on the glass transition and crystallization of pressure-amorphized hexagonal and cubic ice," J. Chem. Phys. **95**, 6849 (1991).

[45]S. Lemke, P. H. Handle, L. J. Plaga, J. N. Stern, M. Seidl, V. Fuentes-Landete, K. Amann-Winkel, K. W. Köster, C. Gainaru, T. Loerting, and R. Böhmer, "Relaxation dynamics and transformation kinetics of deeply supercooled water: Temperature, pressure, doping, and proton/deuteron isotope effects," J. Chem. Phys. **147**, 034506 (2017).

[46]V. Fuentes Landete, L. J. Plaga, M. Keppler, R. Böhmer, and T. Loerting, "Nature of water's second glass transition elucidated by doping and isotope substitution experiments," Phys. Rev. X **9**, 011015 (2019).

[47]P. V. Hobbs, *Ice Physics* (Clarendon Press, Oxford, 1974); V. F. Petrenko and R. W. Whitworth, *Physics of Ice* (Oxford University Press, Oxford, 1999).

[48]C. G. Salzmann, "Advances in the experimental exploration of water's phase diagram," J. Chem. Phys. **150**, 060901 (2019).

[49]A. Rosu-Finsen and C. G. Salzmann, "Benchmarking acid and base dopants with respect to enabling the ice V–XIII and ice VI–XV hydrogen-ordering phase transitions," J. Chem. Phys. **148**, 244507 (2018) and references cited therein.

[50]K. W. Köster, A. Raidt, C. Gainaru, V. Fuentes-Landete, T. Loerting, and R. Böhmer, "Doping-enhanced dipolar dynamics in ice V as a precursor of proton ordering in ice XIII," Phys. Rev. B **94**, 184306 (2016).

[51]K. W. Köster, V. Fuentes-Landete, A. Raidt, M. Seidl, C. Gainaru, T. Loerting, and R. Böhmer, "Dynamics enhanced by HCl doping triggers 60% Pauling entropy release at the ice XII–XIV transition," Nat. Commun. **6**, 7349 (2015).

[52]H. Abe and S. Kawada, "The dependency of dielectric relaxation time on alkali metal ion (Li$^+$, Na$^+$, K$^+$, Rb$^+$) in alkali-hydroxide-doped ice," J. Phys. Chem. Solids **52**, 617 (1991).

[53]K. Amann-Winkel, C. Gainaru, P. H. Handle, M. Seidl, H. Nelson, R. Böhmer, and T. Loerting, "Water's second glass transition," Proc. Natl. Acad. Sci. U. S. A. **44**, 17720 (2013).

[54]S. R. Gough and D. W. Davidson, "Dielectric behavior of cubic and hexagonal ices at low temperatures," J. Chem. Phys. **52**, 5442 (1970).

[55]S. Kawada, "Dielectric anisotropy in ice Ih," J. Phys. Soc. Jpn. **44**, 1881 (1978).

[56]G. P. Johari and E. Whalley, "The dielectric properties of ice I$_h$ in the range 272–133 K," J. Chem. Phys. **75**, 1333 (1981).

[57]M. Tyagi and S. S. N. Murthy, "Dielectric relaxation in ice and ice clathrates and its connection to the low-temperature phase transition induced by alkali hydroxides as dopants," J. Phys. Chem. A **106**, 5072 (2002).

[58]H. Didzoleit, M. Storek, C. Gainaru, B. Geil, and R. Böhmer, "Dynamics of supercooled liquid ammonia hydrate," J. Phys. Chem. B **117**, 12157 (2013).

[59]K. Sasaki, R. Kita, N. Shinyashiki, and S. Yagihara, "Dielectric relaxation time of ice-Ih with different preparation," J. Phys. Chem. B **120**, 3950 (2016).

[60]I. Popov, I. Lunev, A. Khamzin, A. Greenbaum, Y. Gusev, and Y. Feldman, "The low-temperature dynamic crossover in the dielectric relaxation of ice I$_h$," Phys. Chem. Chem. Phys. **19**, 28610 (2017).

[61]C. G. Salzmann, T. Loerting, I. Kohl, E. Mayer, and A. Hallbrucker, "Pure ice IV from high-density amorphous ice," J. Phys. Chem. B **106**, 5587 (2002).

[62]T. M. Gasser, A. V. Thoeny, L. J. Plaga, K. W. Köster, M. Etter, R. Böhmer, and T. Loerting, "Experiments indicating a second hydrogen ordered phase of ice VI," Chem. Sci. **9**, 4224 (2018).

[63]I. Kohl, L. Bachmann, E. Mayer, A. Hallbrucker, and T. Loerting, "Liquid-like relaxation in hyperquenched water at <140 K," Phys. Chem. Chem. Phys. **7**, 3210 (2005).

[64]An example of TTS is given in Fig. 6 of J. Stern, M. Seidl, C. Gainaru, V. Fuentes-Landete, K. Amann-Winkel, P. H. Handle, K. W. Köster, H. Nelson, R. Böhmer, and T. Loerting, "Experimental evidence for two distinct deeply supercooled liquid states of water—Response to 'Comment on 'Water's second glass transition,'" by G. P. Johari, [Thermochim. Acta (2015)]," Thermochim. Acta **617**, 200 (2015).

[65]According to Ref. 9, the ASW samples were sintered by thermally cycling them between 77 and ≈120 K.

[66]G. P. Johari, "Dielectric relaxation time of bulk water at 136–140 K, background loss and crystallization effects," J. Chem. Phys. **122**, 144508 (2005).

[67]Note that the low-temperature dielectric constant of hexagonal ice was previously studied, see, e.g., Refs. 48 and 56–61 and references cited therein. For consistency, in Fig. 3, we show data obtained in the present work.

[68]O. Haida, T. Matsuo, H. Suga, and S. Seki, "Calorimetric study of the glassy state X. Enthalpy relaxation at the glass-transition temperature of hexagonal ice," J. Chem. Thermodyn. **6**, 815 (1974).

[69]C. G. Salzmann, I. Kohl, T. Loerting, E. Mayer, and A. Hallbrucker, "The low-temperature dynamics of recovered ice XII as studied by differential scanning calorimetry: A comparison with ice V," Phys. Chem. Chem. Phys. **5**, 3507 (2003).

[70]C. G. Salzmann, E. Mayer, and A. Hallbrucker, "Thermal properties of metastable ices IV and XII: Comparison, isotope effects and relative stabilities," Phys. Chem. Chem. Phys. **6**, 1269 (2004).

[71]A. Kudlik, S. Benkhof, T. Blochowicz, C. Tschirwitz, and E. Rössler, "The dielectric response of simple organic glass formers," J. Mol. Struct. **479**, 201 (1999).

[72]R. Brand, P. Lunkenheimer, and A. Loidl, "Relaxation dynamics in plastic crystals," J. Chem. Phys. **116**, 10386 (2002) and references cited therein.

[73]A. I. Nielsen, T. Christensen, B. Jakobsen, K. Niss, N. B. Olsen, R. Richert, and J. C. Dyre, "Prevalence of approximate $\sqrt{t}$ relaxation for the dielectric α process in viscous organic liquids," J. Chem. Phys. **130**, 154508 (2009).

[74]The density information is taken from T. Loerting, M. Bauer, I. Kohl, K. Watschinger, K. Winkel, and E. Mayer, "Cryoflotation: Densities of amorphous and crystalline ices," J. Phys. Chem. B **115**, 14167 (2011).

[75]S.-B. Liu, M. A. Doverspike, and M. S. Conradi, "Combined translation-rotation jumps in solid carbon dioxide," J. Chem. Phys. **81**, 6064 (1984).

[76]R. Böhmer and A. Loidl, "Dielectric study of orientational disorder in $(CO_2)_{1-x}(N_2O)_x$ mixed crystals," Phys. Rev. B **42**, 1439 (1990).

[77]K. L. Ngai and M. Paluch, "Classification of secondary relaxation in glass-formers based on dynamic properties," J. Chem. Phys. **120**, 857 (2004).

[78]M. Vogel, P. Medick, and E. A. Rössler, "Secondary relaxation processes in molecular glasses studied by nuclear magnetic resonance spectroscopy," Annu. Rep. NMR Spectrosc. **56**, 231 (2005).

[79]R. E. Hawkins and D. W. Davidson, "Dielectric relaxation in the clathrate hydrates of some cyclic ethers," J. Phys. Chem. **70**, 1889 (1966).

[80]D. W. Davidson, in *Water: A Comprehensive Treatise*, edited by F. Franks (Plenum, New York, 1973), Vol. 2, Chap. 3.

[81]O. Andersson and G. P. Johari, "Nature of the pressure-induced collapse of an ice clathrate by dielectric spectroscopy," J. Chem. Phys. **129**, 234505 (2008).

[82]A "two-phase" behavior for the water kinetics was also found for THF·17D$_2$O doped with 5×10^{-4} KOH, see Fig. 3 of H. Nelson, A. Nowaczyk, C. Gainaru, S. Schildmann, B. Geil, and R. Böhmer, "Deuteron nuclear magnetic resonance and dielectric study of host and guest dynamics in KOH-doped tetrahydrofuran clathrate hydrate," Phys. Rev. B **81**, 224206 (2010).